An Eigenvector Method for the Extraction of Surface Parameters in Polarimetric SAR

Shane R Cloude, Irena Hajnsek*, & Konstantinos P Papathanassiou,

Applied Electromagnetics
11 Bell Street, St Andrews, Fife, Scotland, KY16 9UR
Tel/Fax : ++44 (0) 1334 477598/475570 e-mail :
ael@fges.demon.co.uk

*Deutsches Zentrum für Luft- und Raumfahrt
Institut für Hochfrequenztechnik
1116 Postfach, D-82230 Wessling, Germany
Tel/Fax: ++49(0)815328 2305/1135 e-mail: irena.hajnsek@dlr.de

ABSTRACT - In this paper we introduce a new model for the inversion of surface roughness and moisture from polarimetric SAR data, based on the eigenvalues and eigenvectors of the coherency matrix. We demonstrate how three parameters, namely the polarimetric entropy the anisotropy and the alpha angle can be used in order to decouple roughness from moisture content offering the possibility of a straightforward inversion of these parameters. We investigate the potential of the proposed model using fully polarimetric L-Band ESAR data (DLR) and ground truth measurements from the river Elbe test site.

I. INTRODUCTION

One of the most important applications of scattering polarimetry is in quantitative surface roughness and moisture estimation. In the absence of any simple relationship between scalar reflectivity and surface parameters such as RMS height s, correlation length L, and complex permitivity ε_r, several algorithms have been proposed based on multi-channel polarimetric data. Two main approaches have been employed in the literature based on empirical or semi-empirical relations: scattering amplitude ratio algorithms [1,2] and polarimetric coherence techniques [3,4]. As shown in [5,6] the relationship between surface roughness in scattering polarimetry and the eigenvalues of a coherency matrix have a physical significance in terms of scattering amplitudes and that their ratio represent generalised measures of polarimetric coherence.

A perfectly smooth surface has zero backscatter. However, considering the presence of slight roughness, particularly the case of $ks << 1$ (Bragg scattering), the roughness can be seen as a perturbation of the smooth surface problem. In this case, we obtain the backscatter coefficients for a slightly rough surface using a small perturbation model from Maxwell's equations [3]. According to this model the backscatter from a surface is non-zero and depends on the component of the power spectrum of the surface which matches the incident wavelength and angle of incidence (AOI). The scattering matrix for the surface has the form

$$[S]=\begin{bmatrix} R_S(\theta,\ \varepsilon_r) & 0 \\ 0 & R_P(\theta,\ \varepsilon_r) \end{bmatrix} \quad (1)$$

where the coefficients Rs and Rp are functions of the complex permitivity ε_r and the local incident angle θ

$$R_S = \frac{\cos\theta - \sqrt{\varepsilon_r - \sin^2\theta}}{\cos\theta + \sqrt{\varepsilon_r - \sin^2\theta}}$$

$$R_P = \frac{(\varepsilon_r - 1)(\sin^2\theta - \varepsilon_r(1+\sin^2\theta))}{(\varepsilon_r\cos\theta + \sqrt{\varepsilon_r - \sin^2\theta})^2} \quad (2)$$

The scattering vector in its Pauli-basis representation becomes

$$\vec{k}_P = \begin{bmatrix} R_s + R_P \\ R_S - R_P \\ 0 \end{bmatrix} = m\begin{bmatrix} \cos\alpha * \exp i\phi_1 \\ \sin\alpha * \exp i\phi_2 \\ 0 \end{bmatrix} \quad (3)$$

where m denotes the absolute scattering amplitude. The corresponding coherency matrix results as

$$[T]=\left\langle \vec{k}_P \vec{k}_P^{+} \right\rangle = \begin{bmatrix} \langle |R_S + R_P|^2 \rangle & \langle (R_S - R_P)(R_S + R_P)^* \rangle & 0 \\ \langle (R_S + R_P)(R_S - R_P)^* \rangle & \langle |R_S - R_P|^2 \rangle & 0 \\ 0 & 0 & 0 \end{bmatrix} \quad (4)$$

Note that the angle α, as defined in Equation 3, is independent of roughness, and can be used to extract the dielectric constant if θ is known.

The Bragg scattering model, as addressed in Equations 1-4, predicts zero cross-polarization and zero depolarisation. Real surfaces are characterised by non-zero cross-polarization backscattering as well as by depolarisation effects. However, real rough or smooth surfaces can always be represented in a generalisation of amplitude ratios in terms of their coherency matrix eigenvalue spectrum [7]

$$[T]=\begin{bmatrix}\lambda_1 & 0 & 0\\ 0 & \lambda_2 & 0\\ 0 & 0 & \lambda_3\end{bmatrix} \qquad \lambda_1 \geq \lambda_2 \geq \lambda_3 \qquad (5)$$

By normalising the absolute scattering magnitudes we can interpret them as probabilities pi such that

$$p_1 + p_2 + p_3 = 1 \Rightarrow p_i = \frac{\lambda_i}{\sum \lambda} \qquad (6)$$

Equation 5 provides two parameters to describe the coherence properties of an arbitrary rough surface. One choice of such a pair may be the polarimetric Entropy H and Anisotropy A of the surface, defined as

$$H = -\sum_{i=1}^{3} p_i \log_3 p_i \qquad A = \frac{p_2 - p_3}{p_2 + p_3} \qquad (7)$$

Both parameters varies between 0 and 1. For smooth surfaces, H becomes zero and increases with surface roughness. On the other hand, A can be zero even for rough surfaces, but A > 0 generally indicates the presence of multiple scattering. In the limiting case of one-dimensional surfaces, where HV = 0, A becomes 1. For azimuthally symmetric surfaces, A becomes by definition 0. Figure 1 shows the geometric representation of different rough surfaces in terms of their Entropy and Anisotropy values.

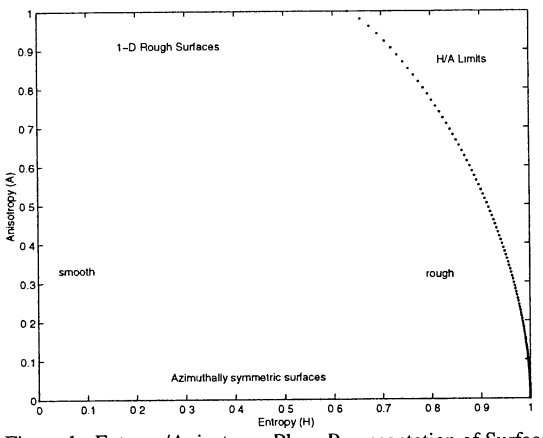

Figure 1 : Entropy/Anisotropy Plane Representation of Surface Scattering

II. POLARIMETRIC SURFACE SCATTERING MODEL

In order to include a non-zero HV backscattering coefficient and depolarisation effects in the Bragg scattering model, we propose a configurational average of the above solution, to obtain a coherence less than one at the same time as generating cross polarized energy. The configurational averaging is taken over a uniform distribution about zero of the surface slope in the plane perpendicular to the scattering plane. If this slope is β, then we propose a uniform distribution of half-width β_1 as shown in Figure 2

$$P(\beta) = \begin{cases} \dfrac{1}{2\beta_1} & |\beta| \leq \beta_1 \\ 0 & \text{otherwise} \end{cases} \qquad (8)$$

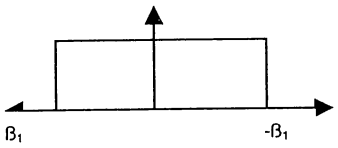

$$0 \leq \beta_1 \leq \frac{\pi}{2}$$

Figure 2 : Uniform Distribution of Surface Slope

Assuming now a non-coherent summation of energy across the distribution of β_1, then the coherency matrix for the surface becomes

$$[T]=\begin{bmatrix} A & B\,\mathrm{sinc}(2\beta_1) & 0 \\ B^{*}\,\mathrm{sinc}(2\beta_1) & C(1+\mathrm{sinc}(4\beta_1)) & 0 \\ 0 & 0 & C(1-\mathrm{sinc}(4\beta_1)) \end{bmatrix} \qquad (9)$$

with sinc(x)=sin(x)/x. The coefficients A B and C expressed in terms of the smooth surface solution are given by

$$A = |R_S + R_P|^2$$
$$B = (R_S + R_P)(R_S^{*} - R_P^{*}) \qquad (10)$$
$$C = \frac{1}{2}|R_S - R_P|^2$$

According Equation 9 both the polarimetric coherence and the level of cross-polarized power is controlled by a single parameter (β_1).

Figure 3 shows the variation of polarimetric coherence (dotted line) and normalised cross-polarized power (solid line). For $\beta_1 = 0$ the HH-VV coherence is unity

and the HV power zero, as expected for the limiting case of a smooth surface, and the coherency matrix becomes the form of Equation 4. As β_1 increases the HV power increases, while the coherence reduces monotonically from 1 for a smooth surface to zero for β_1 = 90 degrees. In this second limiting case of high surface roughness the surface becomes azimuthally symmetric

$$[T]=\begin{bmatrix}\lambda_1 & 0 & 0\\ 0 & \lambda_2 & 0\\ 0 & 0 & \lambda_2\end{bmatrix} \qquad (11)$$

Note that the increase in HV power is faster than the fall off in coherence and so for small β_1 the Anisotropy will be high (close to 1). As β_1 increases so the anisotropy falls monotonically to zero.

Figure 4 shows how this fall in A occurs as a function of β_1. As shown in [6], A loses sensitivity to further increasing roughness above ks = 1. However, for ks < 1 we can see an almost linear relation between A and ks. It is important to note that the value of A at any β_1 is independent of the surface dielectric constant and of the AOI. The variation of A with dielectric constant is also shown to demonstrate the invariance of A to surface material. Similar studies show that A is also independent of the angle of incidence.

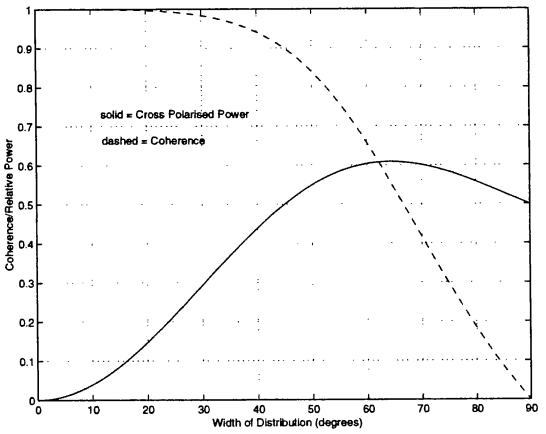

Figure 3 : Variation of Cross-Polarization and Depolarisation with model parameter β_1

We can expose further structure in Equation 9 by plotting the Entropy/Alpha loci of points for dielectric constant ε_r and half-width parameter β_1 for fixed AOI θ. Figure 5 shows the loci for 45 degrees AOI. The loci are best interpreted in a polar co-ordinate system centered on the origin. The radial co-ordinate is then the dielectric constant while the azimuthal angle represents changes in roughness. These loci provide an estimate of the surface dielectric constant, independent of surface roughness. We do this by plotting the entropy/alpha value taken from a coherency matrix [T].

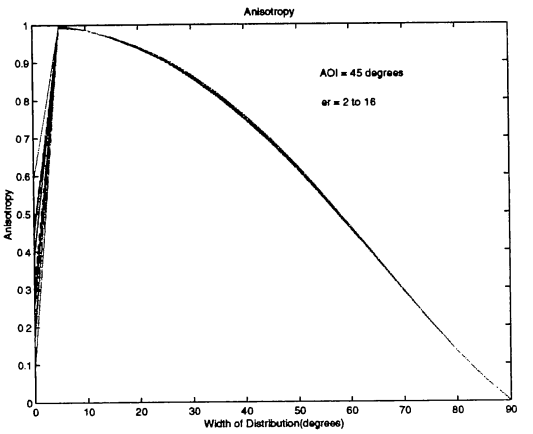

Figure 4 : Variation of Anisotropy with model parameter β_1.

In the limiting case of a smooth surface, this would be a zero entropy point and the alpha would correspond directly to a dielectric constant through Equation 3. However, as the entropy increases so the apparent mean alpha value reduces, causing error in the estimate of dielectric constant. By using Equation 9 we can compensate for this by tracking the loci of constant ε_r, which reduces with increasing entropy. In this way both the entropy and alpha value are required in order to obtain a good estimate of the surface moisture.

Hence, by estimating three parameters, the entropy H, the anisotropy A and the alpha angle α, we obtain a separation of roughness from surface dielectric constant. The roughness estimation comes from A and the dielectric constant estimation from combined H/α values.

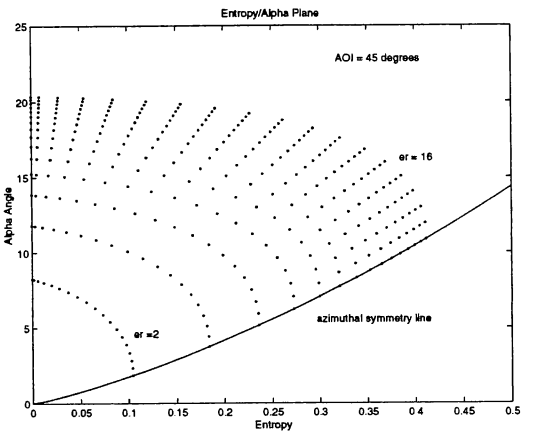

Figure 5 : Entropy/Alpha Diagram for 45 degrees AOI

III. EXPERIMENTAL DATA ANALYSIS

For the validation of the proposed model fully polarimetric L-band data from the Elbe river test site in Germany, acquired by the experimental airborne E-SAR system of DLR in August 1997, are used. Figures 6 and 7 show the HV power image of the test site. During the data acquisition campaign, ground data have been collected over test fields with heterogeneous surfaces. Soil roughness was estimated with a needleboard in four directions: perpendicular and parallel to the ridges, and, perpendicular and parallel to the flight direction. Soil moisture values were measured in depths of 0-4 cm and 4-8 cm using traditional gravimetric sampling and time domain reflectometry (TDR).

Because of the presence of vegetation, only four bare agricultural fields were available for validation. Nevertheless, as the four fields are located at different ranges (covering an incident angle range from 47 up to 52 degrees) with different roughness and moisture values (see Table 1) they are valuable for the validation of inversion results.

Field ID	*ks*	*kl*	ε_r 0-4 cm	ε_r 4-8 cm
A5/10	0.549	1.841	10.79	9.28
A5/13	0.777	2.311	5.34	9.84
A5/14	0.795	3.203	4.51	10.82
A5/16	1.000	3.003	5.86	12.19

Tab. 1: Ground truth values for surface roughness, autocorrelation length and dielectric constant.

After SAR processing and polarimetric calibration, the scattering matrix data are transformed into a covariance matrix form and polarimetrically filtered [8]. Then the eigenvector decomposition is performed, followed by the computation of entropy, anisotropy, and alpha angle [7]. Figures 8,9,10 show the alpha-angle, the entropy and the anisotropy images of the test site respectively. Surface scattering is characterised by a strong dominant scattering mechanism, represented by the first eigenvalue. The amplitudes of the secondary scattering effects, expressed by the second and third eigenvalues, are in comparison very small and therefore, more affected by noise. Thus, in contrast to the entropy, the anisotropy is a more "noisy" parameter especially in low entropy areas as one can see in Figures 9 and 10, and its accurate estimation requires averaging over a large number of samples.

In a pre-selection step, areas where H > 0.45 and alpha > 45 degrees have been masked out in order to select only surface scatterers. For the remaining areas the *ks* values are evaluated directly from their anisotropy values. The result is shown in Figure 12. The correlation between the estimated and measured *ks* values is shown in Figure 13. To reduce the estimation variation (mainly caused by the noisy character of A) the anisotropy A and the alpha angle α have been estimated by averaging a minimum number of 1500 independent samples over each field. The high correlation of about 0.95, and the low RMS error of about 1.5 % underline the performance of the proposed method for roughness estimation.

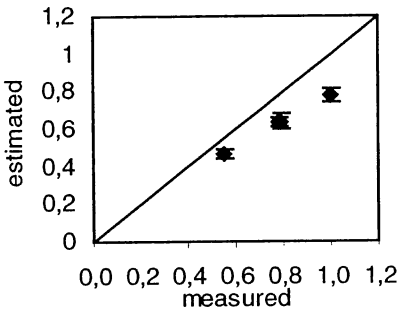

Figure 13: Estimated versus measured surface roughness values.

In a second step, the computed entropy and alpha images are used for the estimation of the dielectric constant. The estimation can be performed directly in terms of a lookup table which delivers the dielectric constant as a function of entropy/alpha values for each range line accounting in this way the variation of incident angle across the image. The resulting ε_r map is shown in Figure 11. The correlation between the estimated and measured values for the four test fields is shown in Figure 14.

From Figure 14 results that the inverted ε_r values correlate better with the ε_r measurements in a depth of 4-8cm than with those measured in 0-4cm.

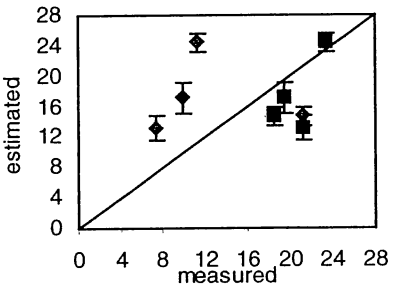

Figure 14: Estimated versus measured dielectric constant. The rhombuses indicate the 0-4 cm depth measurements while the quadrates the 4-8 cm depth measurements.

This is in accordance with the relatively low dielectric constant and the fact of using L-band data. The correlation is about 0.75, and the RMS error lies on the order of 5%. For converting dielectric constant to

volumetric moisture a polynomial relationship from [8] is used. After the polynomial conversion to volumetric moisture the results show the same trend with a correlation about 0.72 and a RMS error about 5% as shown in Figure 15.

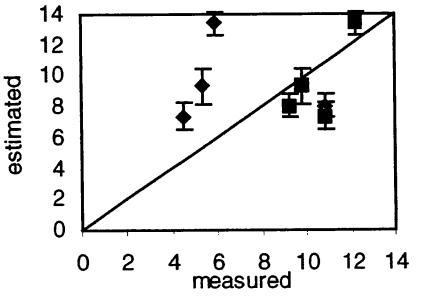

Figure 15: Estimated versus measured volumetric constant. The rhombuses indicate the 0-4 cm depth measurements while the quadrates the 4-8 cm depth measurements.

V. DISCUSSION AND CONCLUSIONS

In this paper we have developed a new general parametric model which enables the quantitative estimation of roughness and dielectric constant for a wide range of natural bare surfaces up to ks = 1 from polarimetric SAR data. The model assumes reflection symmetric surfaces, since by definition the surface normal imposes an orientation axis on the problem. It allows the HH and VV back-scattering coefficients to be different, and includes non-zero HV cross-polarized power as well as depolarisation. The application of the model to experimental data and the overall good agreement between the inverted values for ks, ε_r and μ_v and the ground truth measurements prove that the structure of the data is in agreement with the predictions of the model over a large range of surface conditions.

The main advantage of the proposed inversion model lies in the separation of roughness and dielectric constant estimation which can be performed straightforwardly without the need for any data regression. Further, as the three key observables, the entropy the anisotropy and the alpha angle, are invariant under azimuth rotations the inversion becomes independent on azimuthal slope variations. This makes the application of the technique possible also for terrains with variable topography without the need of any additional topographic information.

Unknown is the influence of surface correlation length, as it is not appearing explicit in the model. Small correlation lengths lead to dihedral scattering effects which biases the alpha angle α estimation increasing the Shh/Svv ratio. This bias can not be removed using the model alone. Fields characterised by eminently different correlation lengths in orthogonal directions, as for example ploughed fields, violate the assumption of a rotation-symmetric roughness term and cannot be resolved by the model. The presence of vegetation cover on the one hand increases the entropy and decreases the anisotropy, leading to overestimation of the surface roughness, and on the other hand increases the alpha angle leading to underestimation of the dielectric constant.

Absolute calibration of the scattering matrix data is not strictly required. While for the ks estimation only cross-talk and relative channel calibration is sufficient, for the estimation of ε_r copolar-phase calibration is essential. The high dependency of the ε_r estimation on the alpha-angle values combined with the fact that any copolar-phase imbalance delta phi affects directly the alpha-angle estimation (delta alpha = delta phi / 2) forces the demand on very accurate phase calibration.

VI. ACKNOWLEDGMENT

This work was performed in the frame of the EC-TMR and ONR-NICOP projects. The authors would like to thank J. S. Lee for filtering the polarimetric coherency matrix data.

VII. REFERENCES

[1] P. C. Dubois, J. J. van Zyl, T. Engman "Measuring Soil Moisture with Imaging Radars", IEEE Transactions on Geoscience and Remote Sensing, Vol.33, pp 916-926, 1995

[2] Y. Oh, K. Sarabandi, F. T. Ulaby "An Empirical Model and an Inversion Technique for Radar Scattering from Bare Soil Surfaces", IEEE Transactions on Geoscience and Remote Sensing, Vol.30, pp 370-381, 1992

[3] M. Borgeaud, J. Noll, "Analysis of Theoretical Surface Scattering Models for Polarimetric Microwave Remote Sensing of Bare Soils", International Journal of Remote Sensing, Vol 15, No. 14, pp 2931-2942, 1994

[4] F. Mattia , T. Le Toan, J. C. Souyris, G. De Carolis, N. Floury, F. Posa, G. Pasquariello, "The effect of surface roughness on multi-frequency polarimetric SAR data", IEEE Trans GE-35, 1997, pp 954-965

[5] S. R. Cloude and K.P. Papathanassiou, "Surface Roughness and Polarimetric Entropy", Proceedings IGARSS'99, pp. 2443-2445, Hamburg, 28 June - 2 July 1999.

[6] S.R. Cloude "Eigenvalue Parameters for Surface Roughness Studies", Proceedings of SPIE Conference on Polarization: Measurement, Analysis and Remote Sensing II, Volume 3754, Denver, Colorado, USA, July 1999

[7] S. R. Cloude, E. Pottier,"An Entropy Based Classification Scheme for Land Applications of Polarimetric SAR", IEEE Transactions on Geoscience and Remote Sensing}, vol. 35, pp. 68-78, 1997.

[8] J.S. Lee, M.R. Grunes, and G. De Grandi, "Polarimetric SAR Speckle Filtering and Its Impact on Classification", Proceedings IGARSS'98, pp. 1038-1040, Singapore, 3-8 August 1997.

[9] G. C. Topp, J. L. Davis and A. P. Annan, "Electromagnetic Determination of Soil Water Content: Measurements in Coaxial Transmission Lines", Water Resources Research, vol. 16, no. 3, pp 574-582, 1980.

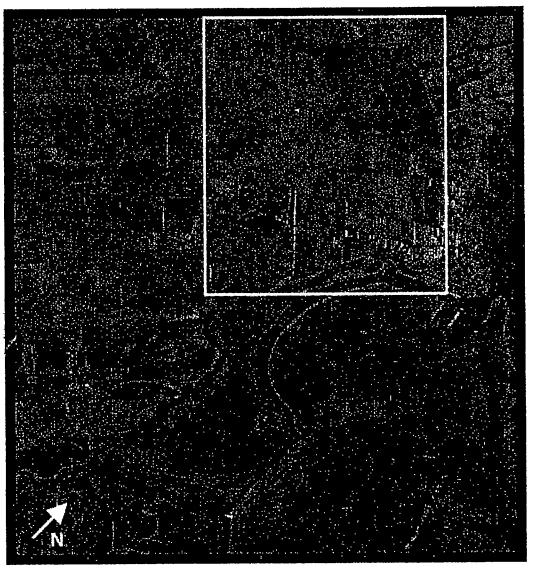

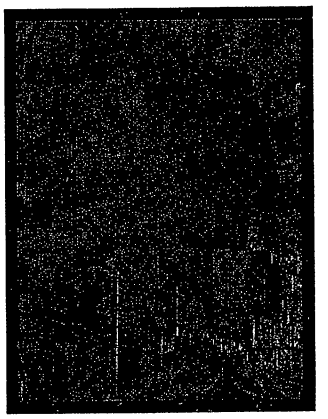

Figure 6: L band power image Elbe River 1997
Figure 7: L band power image Elbe River part 1997

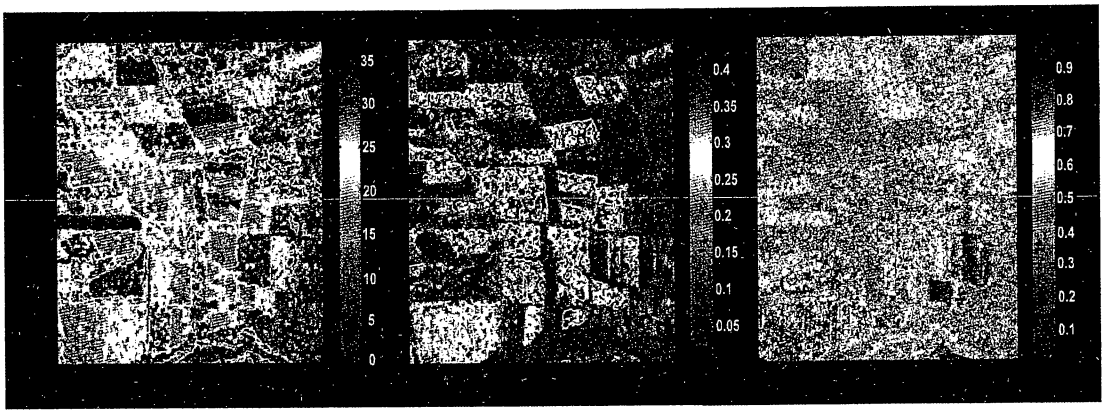

Figure 8: Alpha Angle $\alpha < 43$ degree

Figure 9: Entropy H < 0.5

Figure 10: Anisotropy A < 1

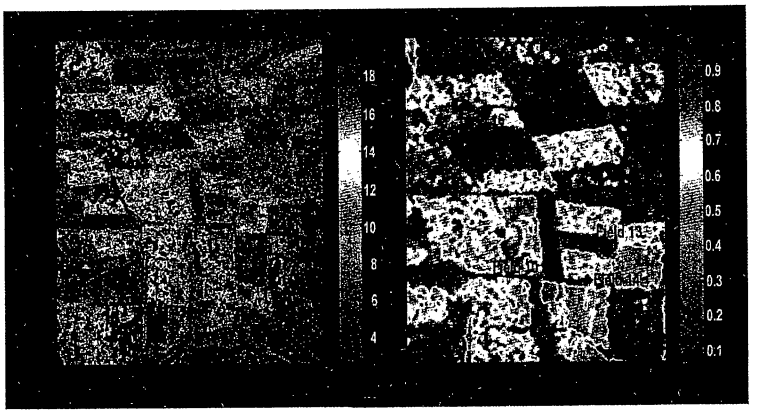

Figure 11: Dielectric constant *er*

Figure 12: Surface roughness *ks*